VII INTERNATIONAL CONGRESS
MOUNTAIN AND STEEP SLOPES VITICULTURE

Extreme viticulture:
from a cultural landscape to an economic and environmental sustainability

11-14 May 2022, Vila Real (UTAD)

Book of Proceedings

EDITED BY: Alberto Baptista and Catarina Cepêda
Universidade de Trás-os-Montes e Alto Douro (UTAD)
Centre for Transdisciplinary Development Studies (CETRAD)

Publisher and Copyright
Universidade de Trás-os-Montes e Alto Douro (UTAD)
1st edition - May 2022, Vila Real

ISBN: 978-989-704-471-7

Extreme viticulture: from a cultural landscape to an economic and environmental sustainability

12-14 May 2022, Vila Real (UTAD)

Book of Proceedings

• • •

EDITED BY: **Alberto Baptista and Catarina Cepêda**
Universidade de Trás-os-Montes e Alto Douro (UTAD)
Centre for Transdisciplinary Development Studies (CETRAD)

All full papers and abstracts submitted to the VII International Congress on Mountain and Steep Sloves Viticulture are subject to a peer review process by selected specialists, experts in the different knowledge areas.
The editors do not bear responsibility for the quality of the English language used by some Auhtors.

This work is supported by national funds, through the FCT – Portuguese Foundation for Science and Technology under the project UIDB/04011/2020.

ISBN: 978-989-704-471-7

Published by: UTAD

Do UAVs help in the detection of grapevine yellows in vineyards that are difficult to reach?

F. Zottele[1], A. Gelmetti[1], B. Mattè[1], P. Crocetta[2]
1 Fondazione Edmund Mach, Centre for Technology Transfer, Italy. fabio.zottele@fmach.it
2 Green Fly di Paolo Crocetta, Italy

Keywords: grapevine yellows, symptoms detection, unmanned aerial vehicles

Abstract. The symptoms of the *flavescence dorée* and *bois noir* are grouped into the so-called Grapevine Yellows (GY). These diseases are affecting viticultural regions worldwide and all varieties and rootstocks seem susceptible but with varying degrees of severity. Typical symptoms include discolouration and necrosis of leaf veins and leaf blades, downward curling of leaves, lack of or incomplete lignification of shoots, stunting and necrosis of shoots, abortion of inflorescences and shriveling of berries. The compulsory control plan for the fight of these diseases includes both the use of insecticides and the eradication of the vines. This latter is part of a monitoring plan of the grapevine yellows that aims to identify outbreaks of the disease and its progression and limit the compulsory phytosanitary control only in the truly affected areas. The identification of the GY is very time-consuming technical work because each vineyard must be visually inspected plant by plant. This type of monitoring is made even more difficult in cases of steeply sloping vineyards and where the vineyard landscape is fragmented. So we raised the following question: is it possible to use UAVs (drones) to remotely monitor the vines that are difficult to reach and identify the grapevine yellows? We present here the results of our field tests made in Trentino (IT) with different drone models (prosumer and professional) and with different types of image acquisition sensors (RGB and multi-spectral).

Introduction

Flavescence dorée is considered to be a quarantine disease in Europe because of its epidemic potential (Directive 77/1993 amended 92/103) and is therefore subject to mandatory procedures for the control of its spread by using pesticides to contain the population of its main insect vector, *Scaphoideus titanus* Ball. (Hemiptera: Cicadellidae) and with the uprooting of every infected vine (*Vitis vinifera* L., Vitaceae).

The symptoms are similar to those of the *bois noir*, but also to the effects of the sting of the *Stictocephala bisonia* Kopp & Yonke (Hemiptera: Membracidae, Buffalo treehopper) which is not related to the two. The visible symptoms of flavescence doreé and bois noir are described as "grapevine yellows" (GY) and appear as early as spring (usually in summer) and are visible until mid-autumn as discolouration and necrosis of leaf veins and leaf blades, downward curling of leaves, lack or incomplete lignification of shoots, stunting and necrosis of shoots, abortion of inflorescences and shriveling of berries (Bovey, 1980). The identification of the GY is a very time-consuming technical work because each vineyard must be visually inspected plant by plant. This type of monitoring is made even more difficult in cases of steeply sloping vineyards and where the vineyard landscape is fragmented. In Trentino (IT) a large part of the wine-growing area is cultivated on steep slopes: the elevation, with a cooler climate, elicits the organoleptic properties of the Chardonnay grapes for bottle-fermented sparkling wine (Champenoise method). However, the areas with the highest altitude are generally also the most difficult to access.

Remote sensing has proven to be effective for determining the health of crops, as stress and deficiencies induce changes in the biophysical and biochemical characteristics of plants that change the optical properties of the plant tissues (Martinelli *et al.*, 2015). Spectral indices are often used in remote sensing, but classic indices (for example, NDVI) are imprecise and alternatives must be found (Albetis *et al.*, 2019). For this reason, we would like to develop a system for remotely sensing the grapevine yellows in real-time without having to first acquire images, process them and interpret them. This system could alleviate the work of the field technicians.

Remote sensing has been successfully applied for detecting Phylloxera, and Esca (Gennaro et al., 2016) using Unmanned Aerial Vehicles (UAVs) rather than satellites because of their practicality in image acquisition (adaptable resolution, no interference with the clouds, rapid deployment...).

A study has recently been proposed for *Flavescence dorée* (Albetis *et al.*, 2019) but our aim is different: we are not interested in identifying the spectral index that discriminates a disease, but to build the first element of an operative, real-time tool for the rapid identification of the Chardonnay vines that exhibit the grapevine yellows for both "*pergola trentina"* and guyot, the two trellis methods used. In the first case, the leaves cover a large part of the vineyard surface, while in the second the vine occupies the surface linearly (Figure 1).

Figure 1. The Unmanned Aerial Vehicle acquiring images over the Chardonnay vineyard. On the left the vines are cultivated with the guyot trellis system, on the right with the *pergola trentina*. The UAV in the image is DJI Matrice 210 RTK V2, equipped with the RGB camera (black) and the MicaSense RedEdge® sensor.

Methods and sources

We selected to operate on a cultivated area in the municipality of Telve Valsugana (46.0400N, 11.5593E). The vineyard, planted with Chardonnay cultivar, is made up of two distinct units by trellis method: guyot (4440 m^2) and pergola (2200 m^2).

On September 5th, 2018, we performed a flight with a DJI Mavic PRO, a prosumer UAV, for the acquisition of RGB images (CMOS ½.3", 12.7 Mpx) and to evaluate, through the use of a virtual reality viewer (DJI Goggles RE, resolution 3840 × 1080 px^2, 70 ms latency), if a senior field technician could remotely inspect the vineyard for detecting the presence of the grapevine yellows in real-time while a certified UAV pilot was managing the flight.

The RGB images collected with a dedicated flight (26.5 m above the take-off point, 8 cm px^{-1} GSD) were ortho-rectified and blended into an orthophoto using the photogrammetric software Pix4dmapper (available at: https://pix4d.com/).

On September 24th, 2019 we conducted another data acquisition campaign: 8 high visibility targets were positioned and planimetric and altimetric coordinates - ground control points - were acquired with a GPS (Leica Geosystems, Leica Zeno 20) with RTK correction provided by the geodetic network of the Province of Trento. Similarly, 21 symptomatic vines (10 guyot, 11 pergola) were identified by the authors and marked on the ground with bright pink spray. Unlike what we did in 2018, we flew with a professional UAV (DJI Matrice 210 RTK V2) with the ability to carry a double payload (two independent image acquisitors), but it also requires a suitable flight license because of the weight (4.91 kg).

The RGB images were collected using a DJI X5s camera (CMOS 4/3", 20.8 Mpx) and the multispectral images have been acquired using a MicaSense RedEdge® sensor in five different wavelengths: Blue (455-495 nm), Green (540-580 nm), Red (658-678 nm), Red-Edge (707-727 nm), and Near Infrared (800 - 880 nm). Pictures of a calibrated reflectance panel (Micasense RP) were captured before and after the two consequent flights on the pergola and on guyot. The elevation of 30 m above the take-off point was fixed for both the flights with both 80% horizontal and vertical overlap among the images.

RGB and multispectral images have been imported in Pix4dmapper to be processed. The RGB image analysis procedure led to the creation of the point cloud and its subsequent densification. Firstly, we generated the orthophoto on which we drew the area covered by 6 randomly chosen vines among all those marked by the surveyors (symptomatic) divided equally between the two trellis systems: pergola and guyot (Figure 2). Similarly, we also selected 6 random asymptomatic vines.

Figure 2. The selected symptomatic vines in the guyot vineyard (left), and in the pergola (right). The soil is partially covered by green grass. The mark (bright pink spray) is partially visible on the third image of the first group.

Theoretical framework and operational concepts

Since we are interested in the reflectance values measured by the multispectral camera on the vine leaves (and not in the values of the soil or the grass) we classified the points that belonged to the ground and the points that belonged to the vegetation (Zahng et al., 2016). The point cloud was further manually pruned outside the study areas. We further decimated the point cloud to obtain a homogeneous density of significant points over the area of interest comparable to the point cloud obtained with the multispectral maps. Lastly, we extracted only the points that fell within the area of competence of the randomly chosen symptomatic and asymptomatic vines and we appended to these points the values read from the 5 band multispectral map. With the measures, we calculated the *Chlorophyll Index* (CI, Steel *et al.*, 2008) and the *Normalized Difference Red-edge Index* (NDRE, Gitelson *et al.*, 2002) - shown in Equation 1 - that proved effective in detecting *Flavescence dorée* in the work of Albetis *et al.* (2019) in case of vines of Chardonnay cultivar that show yellowish discolouration and not reddish colouration.

$$CI = \frac{NIR}{RedEdge} - 1 \qquad NDRE = \frac{NIR - RedEdge}{NIR + RedEdge} \quad \text{Eq. 1}$$

We expect a different behaviour of the values recorded by the multispectral camera between symptomatic and asymptomatic vines, but not between pergola and guyot, we decided to plot the density of the spectral index values of each band in search of signals difference.

We treated each value measured for each band as a realization of a random variable *Y*, and so we looked at the difference in its moments and to limit our research to the first and second-order momentum. Since we expect possible multimodality in the distribution of *Y,* we treated the random variable like a finite mixture model and the identity of each distribution is controlled by a latent categorical variable indicating which mixture component is responsible for the outcome. The model considers K normal distributions with first momentum $\mu_k \in R$ and second momentum $\sigma_k \in R^+$, and each distribution is mixed in proportion λ that lies in the unit K-simplex. For each outcome y_n there is a latent variable z_n that is distributed according to the prevalence parameter λ_k. With these assumptions, the probability distribution *p* of the random variable *Y* becomes:

$$p_Y(y \mid \lambda, \mu, \sigma) = \sum_{k=1}^{K} \lambda_k \mathcal{N}(y \mid \mu_k, \sigma_k)\,. \quad \text{Eq. 2}$$

We used Eq. 2 to infer the parameters of this model using the probabilistic language Stan (Carpenter et al., 2017), a probabilistic programming language that facilitates expression of generative models and full Bayesian inference on parameters therein, using state-of-the-art Hamiltonian sampling procedures with clear failure diagnostics. To complete the model formalization we imposed a generic weakly informative prior on λ_k , μ_k and σ_k, then we run 4 Markow chains, with 1000 iterations for the warm-up and 1000 sampling iterations.

Results

The flight of September 5th, 2018 showed that VR is a promising experimental technology in agriculture, but it is still not enough mature to carry out a real-time service for surveying the emergence of the grapevine yellows. The flight height must be adapted very quickly to capture leaf-scale details and so, maintaining flight altitude of 2 m above the individual vineyards, the inspection execution times were comparable with those of the inspection carried out by a single person on foot. The remote vision is complicated by blurring effects and, at the beginning, by virtual reality sickness. The average resolution of the orthophoto obtained from RGB image processing is 0.008 m. The quality of the final product did not allow the evaluation of the grapevine yellows due to a blur effect in the final raster. Furthermore, although the flight height remained on an average constant, the upper part of the vineyard had a higher Ground Sampling Distance (GSD) than the lower part due to the slope of the vineyard (13.5%).

With a total of 28 minutes of flight (9 min for the pergola, 19 min for the guyot) and with a cloud cover of 7 otka, we collected 139 images for the pergola and 178 for the guyot with a GSD of 1.3 cm px^{-1}. Similarly 462 + 684 multispectral images were acquired with a GSD of 2.5 cm px^{-1}.

The densified point cloud counted 26.336 Mpts (average density 9035.62 pts m^{-2}) on guyot and 20.251 Mpts (average density 8772.11 pts m^{-2}) on pergola. After filtering out the points belonging to the ground, the cloud reduced to 8.812 Mpts (-67%) and 10.114 Mpts (-50%), respectively. The further pruning of the point cloud that focused only on the study area reduced the number of significative points to 4.693 Mpts (-44%) and to 4.413 Mpts (- 56%). The processing of the point cloud led to 1058.25 pts m^{-2} for the guyot and to 2032 pts m^{-2} for the pergola (Figure 3).

The higher density of points over the pergola vineyard is justified by a wider vineleaf coverage masking the ground.

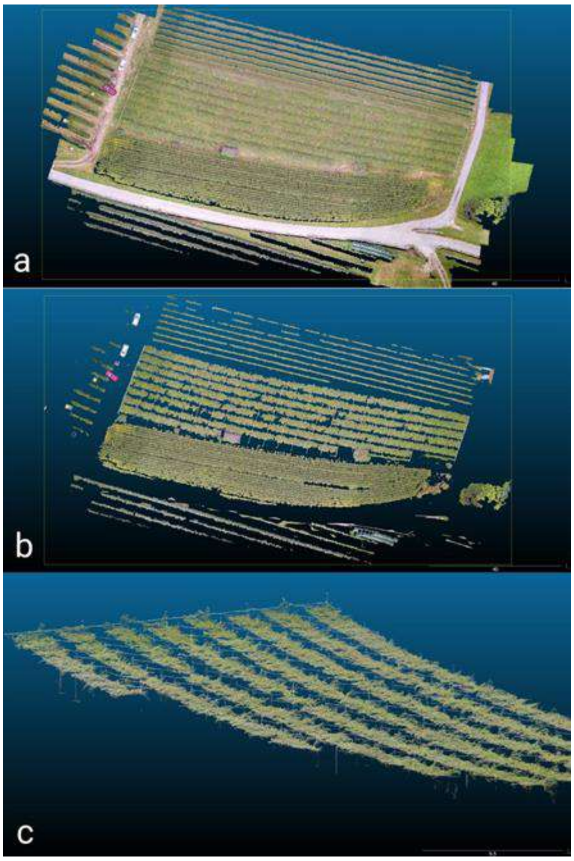

Figure 3. Result of the process for the extraction of the significant points for the RGB cloud. The original point cloud for both guyot and pergola (a), ground-filtered point cloud (b), the leaf coverage of pergola (c).

The distribution of the values of reflectance indices shows us marked multimodality in the non-visible bands (Near infrared and Red Edge), and the derived CI index only (Figure 4).

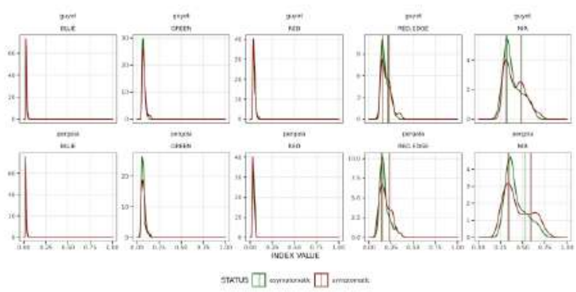

Figure 4. Distributions of the reflectance index for 3 visible (Red, Green, Blue) and 2 non- visible bands (Red Edge and Near Infrared). Green lines represent asymptomatic vines, red lines represent the symptomatics. Vertical lines shown the position of the expected value of the first momentum.

Unlike what is reported in Albetis *et al.* (2019) , the NDRE index does not show differences between symptomatic and asymptomatic vines (Figure 5).

Moreover, the invisible bands show a second peak in the case of diseased vines in the higher values, coherent between pergola and guyot, accentuated in the Near Infrared band. The Hamiltonian Monte Carlo algorithm ran without problems, the metrics for the evaluation of the sampling efficiency, R-hat, and the effective sample size per iteration, gave reasonable results and all the iterations of the Markov chain ended without divergences.

We found that the three indices work differently. The Red Edge band discriminates based on mixing ratios (λ_1), while the NIR band is effective in discrimination using the expected values of the first moment, $E\,[\mu_2]$. Similarly, in the case of CI, the expected value of the first moment seems to be an effective parameter in discrimination, but the mixing ratios are not concordant between pergola and guyot. NDRE showed no particular ability to discriminate symptomatic and asymptomatic vines. Probably, the combination of the two colour bands dilutes the discriminatory capacity rather than enhancing it. This effect merits further investigations.

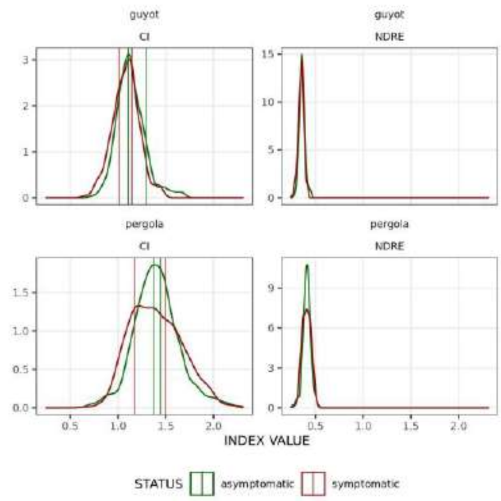

Figure 5. Distribution of the derived indexes (Chlorophyll Index, CI and Normalized Difference Red Edge Index, NDRE). Green lines represent asymptomatic vines, red lines represent the symptomatics. Vertical lines shown the position of the expected value of the first momentum.

To build an automatic and real-time system for the identification of Grapevine Yellows, it is, therefore, possible to work with just only one colour band (in the not visible spectrum) thus avoiding the use of compound indices and post-processing.

The expected values of the first and second momentum (μ_2,σ_2) of the second peak and the mixing values (λ_k) of the gaussian mixtures are shown in Table 1.

Table 1. Expected values of the second location parameter and mixing ratio of the two non-visible colour (RE stands for Red edge) bands and of the Clorophill Index (CI) for symptomatic (+) and asymptomatic (-) vines, over pergola and over guyot.

index		guyot			pergola		
		μ_2	λ_1	λ_2	μ_2	λ_1	λ_2
RE	-	0.22	0.44	0.56	0.22	0.58	0.42
	+	0.22	0.37	0.63	0.24	0.54	0.46
NIR	-	0.49	0.57	0.43	0.52	0.56	0.44
	+	0.48	0.41	0.59	0.59	0.55	0.45
CI	-	1.33	0.84	0.16	1.46	0.54	0.46
	+	1.18	0.60	0.40	1.53	0.34	0.66

Conclusions

With our tests, we have shown how a professional drone equipped with an RGB camera and a multispectral camera can, in perspective, become an effective tool to identify the GY for both pergola and guyot. However, some aspects remain to be explored for future improvements.

In our opinion, the service to detect GY must be a real-time analysis (i.e. without post-processing) of images that just runs as the data are collected (on-line streaming during the flight).

So, what we have shown with this work is promising: the discrimination criteria can be delegated to a single colour band in the spectrum of the non-visible (Red Edge or NIR).

Nevertheless, the response in terms of reflectance of symptomatic plants needs to be further investigated. For this reason, if the project proceeds, it would be appropriate to focus on newly acquired images and evaluate, through a model similar to the one used, but hierarchical, the inter-vines variability of the reflectance indices. In this way, we expect to assemble an information library to support the analysis of the data acquired while the UAV is flying. This perspective is plausible as drones mount increasingly powerful GPU-based Inertial Measurement Units (IMU) that could be used for the analysis of the values acquired in real-time (Lee *et al.*, 2017).

On the other hand, we are witnessing a constant development of new optical sensors at higher resolutions and lower costs. Reducing the number of bands to be acquired would certainly simplify the machinery and would reduce the total weight. Lastly, multispectral sensors with higher resolution would allow flying at higher altitudes, allowing faster flight and an increase in the surveyed area, and a richer point cloud.

Based on our experience, an important step to set up a real-time service with on-line analysis of the steamed images is the real-time identification of the single vines. The algorithms we tested (only in the post-processing of the images) cannot effectively identify the individual vines neither in the case of the guyot, whose configuration of the leaf cover assumes the characteristics of a continuous wall of leaves nor in the case of the pergola. This is due to two main reasons: the spacing of the vines is very narrow (especially in guyot) and the soil is almost uniformly covered by grass: the herbaceous canopy shows colours similar to those of the vine both in the visible and in the invisible spectrum. Techniques for identifying plants based on artificial intelligence have recently been proposed (Ampatzidis and Partel, 2019).

We should then understand why the composite indices (for example, the NDRE) have not shown an efficacy equal to that in our expectations in identifying the Grapevine Yellows. Differently from (Albetis *et al.*, 2019), our case deals with just a white-berry grapevine cultivar (Chardonnay) whose symptoms are the yellowish and not the reddish of the leaves, and because we focused on discriminating the symptoms not by Cultivars, but for two different trellis methods. It is then conceivable to try further compound indices such as the Red-Edge Green Index (REGI), the Green Normalized Difference Vegetation Index (GRVI, Gitelson *et al.*, 2002) and the Normalized Pigment Chlorophyll Index (NPCI, Zarco-Tejada *et al.,* 2001). The analysis of these indices would help to further strengthen the choice of just one colour band - or a very narrow band- in the spectrum of the non-visible.

However, a word of caution should be spent regarding the costs of the monitoring system: the cost of the drone (~10 kEUR) and the multispectral camera (~10 kEUR) and the training of the pilot enabled to fly with professional drones is still high compared to the economic benefit. Nevertheless, given that we are still in the early stages of the investigation and that obtaining an effective and efficient service could still entail a few years of development, we expect a significant reduction in costs over time to obtain the necessary capital.

The FLAG-vite project was entirely funded by the Mach Foundation (OI-P1825018I) for the 2018-2019 period. Our thanks go to the all Pix4d support staff (Alice Bonfiglio, Kapil Khanal and Momtanu Chakraborty) for their help in solving some problems encountered in the image processing steps, and to prof. Fernando Maines of the Training and Education Centre for having kindly lent the GPS-RTK for this field survey. Thanks to Claire Bauling for proofreading the article. Finally we would like to thank the Stan community - and especially Bob Carpenter and Mike Lawrence - for useful discussions and helpful criticism.

References

Albetis, J.; Jacquin, A.; Goulard, M.; Poilvé, H.; Rousseau, J.; Clenet, H.; Dedieu, G.; Duthoit, S. (2019) On the Potentiality of UAV Multispectral Imagery to Detect *Flavescence dorée* and Grapevine Trunk Diseases. *Remote Sens.*,11, No 1: 23.

Ampatzidis, Y.; Partel, V. (2019) UAV-Based High Throughput Phenotyping in Citrus Utilizing Multispectral Imaging and Artificial Intelligence. *Remote Sens.* No 11: 410.

Bovey, A. (1980). Maladies á virus et affections similaires de la vigne. France. La Maison rustique.

Carpenter, B., Gelman, A., Hoffman, M., Lee, D., Goodrich, B., Betancourt, M., Brubaker, M., Guo, J., Li, P., Riddell, A. (2017). Stan: A Probabilistic Programming Language. *Journal of Statistical Software, 76*(1), 1 – 32.

Gennaro, S.F.D.; Battiston, E.; Marco, S.D.; Facini, O.; Matese, A.; Nocentini, M.; Palliotti, A.; Mugnai, L. (2016) Unmanned Aerial Vehicle (UAV)-based remote sensing to monitor grapevine leaf stripe disease within a vineyard affected by esca complex. *Phytopathol. Mediterr.* No 55: 262–275.

Gitelson, A.A.; Kaufman, Y.J.; Stark, R.; Rundquist, D. (2001) Novel algorithms for remote estimation of vegetation fraction. *Remote Sens. Environ.* No 80: 76–87.

Lee, J., Wang, J., Crandall, G., Šabanović, S., Fox, G. (2017). Real-Time, Cloud-Based Object Detection for Unmanned Aerial Vehicles. *First IEEE International Conference on Robotic Computing (IRC)*, Taichung, 2017: 36-43.

Martinelli, F.; Scalenghe, R.; Davino, S.; Panno, S.; Scuderi, G.; Ruisi, P.; Villa, P.; Stroppiana, D.; Boschetti, M.; Goulart, L.R.; et al. (2015) Advanced methods of plant disease detection. A review. *Agron. Sustain. Dev.* No 35: 1–25.

Steele, M.R.; Gitelson, A.A.; Rundquist, D.C. (2008) A comparison of two techniques for nondestructive measurement of chlorophyll content in grapevine leaves. *Agron. J.* No:100: 779–782.

Zhang, W.; Qi, J.; Wan, P.; Wang, H.; Xie, D.; Wang, X.; Yan, G. (2016) An Easy-to-Use Airborne LiDAR Data Filtering Method Based on Cloth Simulation. *Remote Sensing.,*No 8(6):501.

Zarco-Tejada, P.J.; Miller, J.R.; Noland, T.L.; Mohammed, G.H.; Sampson, P.H. (2001) Scaling-up and model inversion methods with narrowband optical indices for chlorophyll content estimation in closed forest canopies with hyperspectral data. *IEEE Trans. Geosci. Remote Sens*. No 39: 1491–1507